Cognitive Neurodynamics (2021) 15:835–845
https://doi.org/10.1007/s11571-021-09671-4

RESEARCH ARTICLE

Morphological analysis of subcortical structures for assessment of cognitive dysfunction in Parkinson's disease using multi-atlas based segmentation

S. Sivaranjini[1] · C. M. Sujatha[1]

Received: 11 September 2020 / Revised: 27 January 2021 / Accepted: 25 February 2021 / Published online: 14 March 2021

Abstract
Cognitive impairment in Parkinson's Disease (PD) is the most prevalent non-motor symptom that requires analysis of anatomical associations to cognitive decline in PD. The objective of this study is to analyse the morphological variations of the subcortical structures to assess cognitive dysfunction in PD. In this study, T1 MR images of 58 Healthy Control (HC) and 135 PD subjects categorised as 91 Cognitively normal PD (NC-PD), 25 PD with Mild Cognitive Impairment (PD-MCI) and 19 PD with Dementia (PD-D) subjects, based on cognitive scores are utilised. The 132 anatomical regions are segmented using spatially localized multi-atlas model and volumetric analysis is carried out. The morphological alterations through textural features are captured to differentiate among the HC and PD subjects under different cognitive domains. The volumetric differences in the segmented subcortical structures of accumbens, amygdala, caudate, putamen and thalamus are able to predict cognitive impairment in PD. The volumetric distribution of the subcortical structures in PD-MCI subjects exhibit an overlap with the HC group due to lack of spatial specificity in their atrophy levels. The 3D GLCM features extracted from the significant subcortical structures could discriminate HC, NC-PD, PD-MCI and PD-D subjects with better classification accuracies. The disease related atrophy levels of the subcortical structures captured through morphological analysis provide sensitive evaluation of cognitive impairment in PD.

Keywords Magnetic resonance imaging · Parkinson's disease · Cognitive impairment · Morphology · Multi-atlas segmentation

Introduction

Parkinson's disease (PD) is a chronic and severe neurodegenerative disorder. PD is related to loss of dopaminergic neurons in substantia nigra and other susceptible regions of brain, though the etiology of the disease is not clear (Poewe et al. 2017). This degeneration is characterised by onset of cardinal motor symptoms such as slow movements, tremor and muscular rigidity (Dauer and Przedborski 2003). In addition, early stages of the disease are often associated with non-motor symptoms including cognitive deficits, anxiety, hallucinations, and olfactory dysfunctions (Chaudhuri et al. 2006; Simuni et al. 2018). Cognitive functional impairment is a significant clinical manifestation in PD and is related to the cholinergic neurons along with the dopaminergic neurons and other neurotransmitter systems where the diffuse nerve degeneration results in neuropathological changes (Aarsland 2016; Dadar et al. 2018). Recent neuroimaging studies showed prevalence of mild cognitive deficits in 40% of PD patients at the time of initial diagnosis which eventually develops into dementia (Wolters et al. 2020). Mild cognitive impairment in early stage PD has an increased risk of progressing to dementia at the later stages of the disease (Aarsland 2016; Litvan et al. 2011). The cortical and limbic Lewy body pathology is also reported to be causative for cognitive decline in PD, but the hypothesis still remains controversial (Chaudhuri et al. 2006). Clinical understanding of cognitive function in early stage PD may

✉ S. Sivaranjini
sivaranjinipragasam@gmail.com

[1] Department of Electronics and Communication Engineering, College of Engineering (CEG), Anna University, Chennai, India

provide prognostic insight into its pathophysiology and may aid in timely therapeutic intervention.

The cognitive functions are investigated in several neurological studies through clinical assessments such as Montreal Cognitive Assessment (MoCA) (Nasreddine et al. 2005), Mini Mental State Examination (MMSE) (Folstein et al. 1975), Clinical Dementia Rating (CDR) (Hughes et al. 1982) and the Geriatric Depression Scale (GDS) (Yesavage et al. 1983). Mild cognitive impairment in PD is initially connected to executive, attention and visuospatial functions. MoCA consistently shows stronger sensitivity for assessment of executive functions involving reasoning and planning. The Parkinson Study Group Cognitive/Psychiatric working Group and Movement Disorder Society has endorsed MoCA as global cognitive function assessment method clinically (Chou et al. 2010) and as a level 1 diagnostic tool for MCI in PD (Kletzel et al. 2017; Litvan et al. 2011). MoCA as a global cognition assessment instrument shows an acceptable discriminating capability in the detection of MCI in PD (Hoops et al. 2009).

Studies have reported evidence of gray and white matter changes associated with cognitive decline in PD (Amoroso et al. 2018; Hopes et al. 2016; Salvatore et al. 2014). The structural changes that reflect the neuropathology of PD are well captured through neuroimaging techniques (Provost et al 2015). The morphological changes that could predict an increased risk of cognitive impairment in PD can be obtained through Magnetic Resonance Imaging (MRI). Morphological studies have shown that PD-MCI exhibited a wider range of gray matter volume reductions in the frontal lobe, temporal lobe structures such as the hippocampus, amygdala and parahippocampal gyrus (Garg et al. 2015; Rektorova et al. 2014). The pattern of gray matter loss is more diverse in MCI; however, the progression of volume loss may be accelerated when dementia begins (Babu et al. 2014). Cortical gray matter changes are more pronounced and widespread in PD-Dementia compared with non-demented PD-MCI patients. However, the significant reductions in gray matter volume have not consistently been found in PD-MCI (Hall and Lewis 2019). The clinical heterogeneity of PD demands efficient methods to detect subtle changes in the brain structures and their local anatomical variations through MR images at voxel levels.

Whole brain segmentation is essential to capture volumetric alterations facilitating the quantitative analysis for pathology characterization (Heckemann et al. 2006). Automatic segmentation is one of the main challenges in medical image analysis due to overlap in signal properties among anatomically distinct structures. Atlas-based segmentation is one of the most significant approaches that utilize the spatial correspondence between reference atlas and target images. A multi-atlas strategy, where each available atlas is used to compute an estimate of the segmentation of the target image is found to be robust. However, multi-atlas segmentation requires large number of atlases, which when compensated, results in local anatomical variations. Patch based method is able to overcome this limitation with the combination of multi-atlas segmentation and label fusion.

Recently, deep neural networks have been utilized to learn a multi atlas segmentation model which predicts the class label of each voxel by providing a local region around that voxel (Milletari et al. 2017). The image patches used for the parcellation of tissues into anatomical units are trained through convolutional neural networks to improve the localization accuracy and spatial consistency in the MR images. The learning task in whole brain segmentation is simplified to localized sub-tasks using multiple networks, with each network implemented to learn sub-space in a standard MNI atlas space (Bermudez et al. 2019). The extraction of volumetric features allows quantification of structural variations of the subcortical regions and aid in clinical investigation of PD.

The aim of this work is to investigate the morphological changes in subcortical regions of PD subjects with mild and severe cognitive impairment using spatially localized multi atlas segmentation model with subsequent volumetric analysis. Texture features obtained from the significant regions are applied to an ensemble subspace k-nearest neighbour (kNN) classifier to postulate a better classification performance.

Methods

Subjects

The data utilised in this study is obtained from Parkinson's Progression Markers Initiative (PPMI) database. PPMI is a multi-site longitudinal cohort study of de novo and drug-naïve PD subjects along with age matched healthy control group (Marek et al. 2011). The tracking of disease progression is possible through the longitudinal data available in PPMI study. The assessment of cognitive function in PD subjects is implemented with MoCA scores. The T1 MR images of 58 Healthy Control subjects taken at baseline and 135 PD subjects prospectively followed up from baseline to a year are used in this study. The selection criterion based on MoCA scores (Chaudhary et al. 2020; Chou et al. 2010; Hoops et al. 2009) includes 58 HC and 91 PD subjects with scores greater than 25 (represented as NC-PD) and 44 PD subjects with scores less than 26. The 44 PD subjects are further categorised into 19 Parkinson's disease—Dementia subjects with MoCA scores of less than 24 and the remaining 25 subjects as Mild Cognitive

Impairment Parkinson's disease subjects. T1 MR images with voxel spacing of $1 \times 1 \times 1$ mm^3 and matrix of $240 \times 256 \times 176$ are selected. The demographic details of the subject groups used in this study are given in Table 1.

Segmentation

The proposed flow diagram for the analysis of cognitive functions in PD is shown in Fig. 1. MR images of HC and PD subjects are subjected to whole brain segmentation using spatially localized atlas network tiles segmentation method (Huo et al. 2019) and the features extracted from selected subcortical regions of interest are subjected to classification using ensemble classifier.

Prior to segmentation, all the input images are subjected to pre-processing which includes registration, bias field correction and intensity normalisation (Huo et al. 2018). All the images are registered to MNI305 template using affine transformation (Evans et al. 1993). The intensity inhomogeneity correction of the registered images is performed using N4 bias field correction (Tustison et al. 2010). The intensities of the corrected images are normalised by regression based intensity normalisation. The image intensities are subtracted with mean intensity and normalized by standard deviation. 45 manually labelled T1 MR images from Open Access Series on Imaging Studies dataset (Marcus et al. 2007) are used as the training data atlases and 5111 multi-site scans are used as auxiliary training data. A binary mask generated by thresholding the average of brain tissue labels of 45 training atlases, is used to eliminate the non-brain regions. The normalized volume is obtained from the pre-trained regression model built from mean sorted intensity vector of the atlases and the brain regions of MR images.

The normalized volume mapped to a standard MNI atlas space is subjected to whole brain segmentation using a set of independent 3D U-Net networks by adopting an overlap-tile strategy (Çiçek et al. 2016). The subspaces of the brain volume are used as input to the 3D U-Net. Multiple networks are used to learn contextual information of patches at different spatial locations. Each network tile overlapped in the subspace learns from similar parts of the brain regions with smaller spatial variations. The nth sub-network covers the subspace ψ_n with one coordinate (x_n, y_n, z_n), where the size of every subspace $(d_x, d_y, d_z), n \in \{1, 2, \ldots k\}$ used in the network architecture is given as

$$\psi_n = \left[x_n : (x_n + d_x), y_n\left(y_n + d_y\right), z_n(z_n + d_z)\right] \quad (1)$$

The number of network tiles is determined by the factor $k = 3 \times 3 \times 3$, thus covering the entire MNI space with 27 independent overlapped 3D U-Nets. The U-Net architecture consists of a contracting path to capture context and a symmetric expanding path that enables precise localization. The contracting path consists of two $3 \times 3 \times 3$ convolutions with a Rectified Linear Unit (ReLU) for each layer, followed by $2 \times 2 \times 2$ max pooling with strides of two in each dimension. In the expansive path, each layer consists of a stride two upconvolution of $2 \times 2 \times 2$ in each dimension, followed by two $3 \times 3 \times 3$ convolutions each with a ReLU. At the final layer, a $1 \times 1 \times 1$ convolution is used to map each feature vector to the desired anatomical labels.

Each training data set comprising 45 manual atlases and 5111 auxiliary atlases is accompanied by a set of neuroanatomical labels, where every voxel is coded as one of 133 anatomical structures. The output of each 3D U-Net is made compatible to obtain the 133 output labels as given in the manually segmented MR images utilised in training the network. The multiple U-Nets corresponding to overlapped subspaces provide more than one segmentation results for a single voxel of a target image. Hence, majority vote label fusion is used to combine 27 segmentations from network tiles to yield the final segmentation in MNI space as

$$S_{MNI}(i) = \underset{l \in \{0,1 \ldots L-1\}}{\arg\min} \frac{1}{k} \sum_{m=1}^{k} p(l|S_m, i) \quad (2)$$

where l represents the possible labels for a given voxel. The final label fused segmentation is inversely registered to the original space using affine registration.

The subcortical structures associated with the cognitive dysfunctions in PD are selected from labelled brain regions based on their Cohen's d values and their volumetric alterations are further analysed using Gray Level Co-occurrence Matrix (GLCM). The selected 10 subcortical structures include: the accumbens area, amygdala, caudate, putamen and thalamus proper of both the right and left hemispheres. The textural features from the selected regions of interest are subjected to classification using ensemble of a subset of kNN classifiers.

Table 1 Demographic details and group characteristics:

	HC (n = 58)	NC-PD (n = 91)	PD-MCI (n = 25)	PD-D (n = 19)	*p* value
Gender (M:F)	36:22	57:34	17:8	16:3	0.304
Age (in years)	56.97 ± 11.29	58.71 ± 9.50	63.64 ± 7.08	65.58 ± 8.88	< 0.001
MoCA	28.55 ± 1.22	28.14 ± 1.37	24.68 ± 0.47	20 ± 2.40	< 0.001
UPDRS	0.87 ± 0.47	20.97 ± 9.18	26.72 ± 12.53	22.78 ± 13.08	0.047

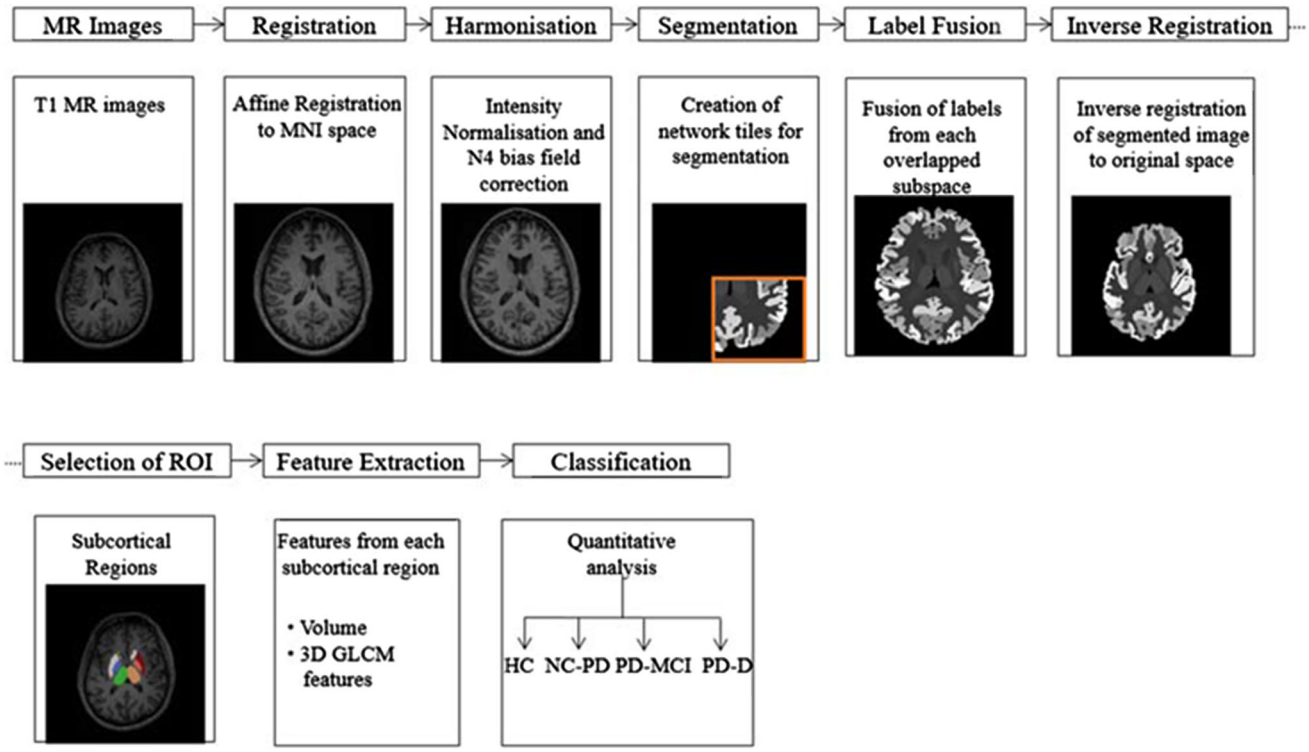

Fig. 1 Process flow diagram for the analysis of Parkinson's disease

3D-GLCM features

Gray level co-occurrence matrix is calculated in different directions to extract the spatial variations that may be associated with PD related cognitive decline. The local features are computed at each point to obtain latent information from the brain regions. Haralick texture features are calculated from 3D GLCM in 13 directions with 4 distances from the neighbourhood pixels (Liu et al. 2013). A total of 10 Haralick GLCM features that include energy, entropy, contrast, homogeneity, variance, sum mean, cluster shade, cluster tendency, max probability, inverse variance are extracted from the segmented subcortical regions. The averaged 3D texture features in all the 13 directions are utilised for the analysis of PD subjects.

Classification

An ensemble of a subset of kNN classifiers is used to differentiate HC and PD subjects with MCI and dementia. Ensemble classifier utilises an n number of kNN classifiers to improve the predictive performance of the classifier. A random sample of features m are drawn without replacement from the entire feature set d and a kNN classifier is trained with those random predictors obtained from m (Gul et al. 2018). The kNN classifiers, anchor n points for the given classes and choose the centroids from the n points based on the Euclidean distance measure. Each point in the feature vector is mapped to the nearest centroid to form clusters (Ho 1998). Thus each classifier is trained on an iterative process until the highest accuracies are obtained from the ensemble of classifier. The classifier employs random subspace to ensemble the resultant values and provide classification results with higher performance. A tenfold cross validation scheme with 30 learners and 5 subspace dimensions has been used in this work. The performance of the classifier is analysed through accuracy, specificity and sensitivity metrics. A mean accuracy is obtained from the proportions of true positive and true negatives of the four classes to give the total number of predictions that are correct. A weighted average sensitivity is calculated from the proportion of true positives in each class. Similarly the weighted average specificity is determined from the proportion of true negatives correctly classified as negative.

Results

The T1 MR images of HC, PD disease subjects with and without dementia are used to extract the volumetric alterations of brain regions. The representative set of MR images for each subject group, the corresponding pre-processed and segmented images are shown in Fig. 2. The pre-

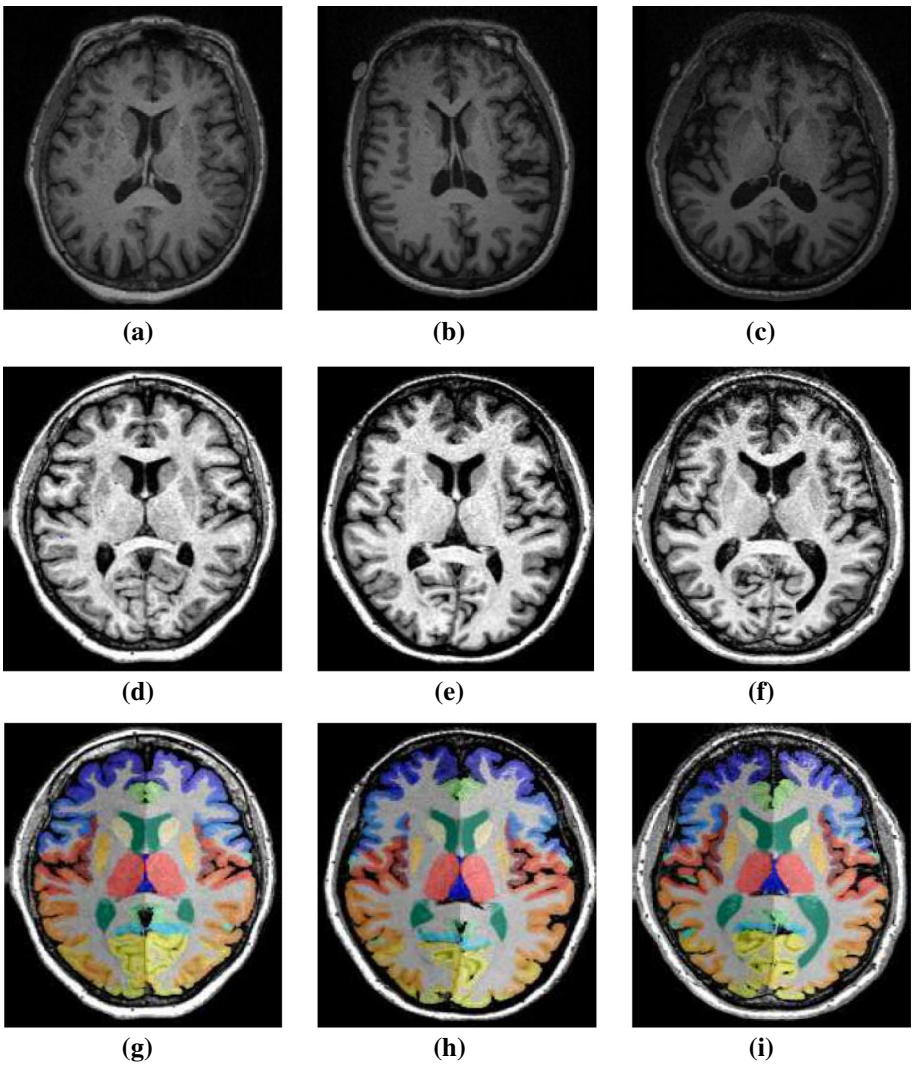

Fig. 2 Representative set of **a**–**c** raw MR images of healthy control, PD-MCI and PD-D subjects, **d**–**f** pre-processed MR images, **g**–**i** segmented MR images

processed MR slices that depict a clear view of the anatomical structures are chosen for representation. The variability in the brain regions appear reduced in the pre-processed non-uniformity corrected images captured with suitable parameters. An optimum coefficient of variation bias filed correction was applied with respect to a convergence threshold of 0.001, for 50 iterations with 0.15 full width half maximum convolution kernel.

The 132 anatomical regions are segmented from the MR images using multi-atlas segmentation method, excluding the background label obtained from segmentation. The volumes of each segmented region are acquired to analyse the structural variations in PD subjects. The segmented volumes are normalised to derive the Total Intracranial Volume (TIV) for the HC, PD-MCI and PD-D groups (Fig. 3). Volumetric changes of the brain are observed to be minimal in the subject groups based on the median TIV range. The normalized TIV is found to be slightly lower for PD-D group when compared with the HC subjects that

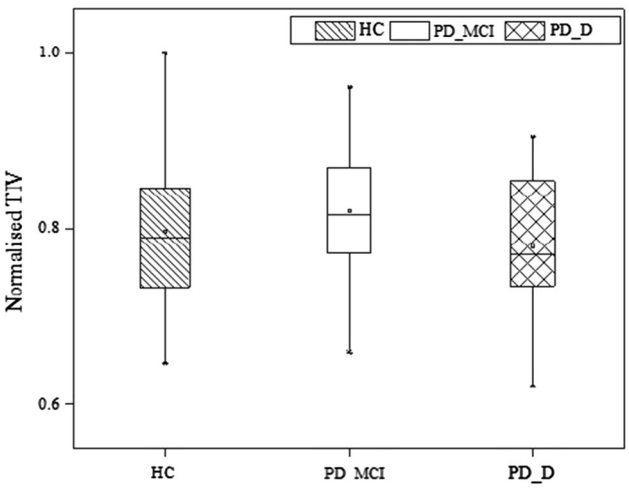

Fig. 3 Box graph representation of normalised TIV mean values of HC, PD-MCI and PD-D subjects groups

could be attributed to the atrophy levels in PD. The variation in TIV is not consistent with the PD-MCI subject group.

The disease related atrophy of the segmented anatomical regions is evaluated using absolute effect size index called Cohen's d value. The volumetric differences in the subcortical regions of various subject groups are categorised as small, medium and large effect sizes based on these indices. The regions that exhibit medium and large effect sizes in the PD-D subject groups with HC are given in Table 2.

PD-MCI subjects show relatively lower volumetric differences as evidenced by the Cohen's d values with only a mediocre effect size in the caudate region ($p = 0.05$). The PD-D subject group shows volumetric differences with greater significance ($p = 0.001$) in the Accumbens with very large absolute effect size. Similarly, higher significance with potential medium effect size is observed in putamen ($p = 0.004$) and thalamus ($p = 0.005$). Amygdala ($p = 0.05$) and caudate ($p = 0.052$) show considerable effect size with comparatively lesser significance in the PD-D subject group. The progression of disease from MCI to PD-D is evidenced through mediocre effect size in accumbens, amygdala and thalamus. The NC-PD subjects show large effect size ($p < 0.05$) in the significant subcortical regions when compared with PD-D group and small effect size with the HC group.

The volumetric estimates of the subcortical structures with medium and large effect sizes, which include accumbens, amygdala, caudate, putamen and thalamus of both the hemispheres are obtained for HC, PD-MCI and PD-D subjects (Fig. 4). Minimal change in the subcortical volumes of the PD-MCI group is seen with an overlap in the volumetric estimates of the HC subjects. An overall reduction in the median range of the subcortical volumes is found in PD-D subjects compared with the HC subjects. The significant volumetric reduction in the subcortical regions could be attributed to the disease progression in the PD-D subjects.

The morphological alterations of the subcortical structures are further analysed using 3D GLCM. The mean Haralick texture features obtained from the subcortical regions are averaged for 13 directions for each class. Significant differences ($p < 0.05$) in the feature values are found between any two class combination in the right accumbens area, left accumbens area, right amygdala, right caudate, left caudate, right putamen, left putamen, right thalamus and left thalamus. Analysis of variance through ANOVA over energy, entropy, homogeneity, max probability and inverse variance shows greater significance ($p < 0.05$) in differentiating the three classes.

The average values of 5 significant features for the 9 significant subcortical regions are shown in Fig. 5. Entropy and inverse variance present a trend of increase in the first 5 significant subcortical regions and a decrease in the other regions. The trend of increment and decrement reverses for energy, homogeneity and max probability. This shows a constant pattern of textural variations in the significant subcortical regions. The ensemble subspace kNN classifier is trained with all the features of the 9 significant subcortical regions and the performance of the classifier is analysed for differentiating the three classes. The performance of the classifier is analysed for each subject group as HC versus PD-MCI, HC versus PD-D, NC-PD versus PD-D and PD-MCI versus PD-D is shown in Table 3.

Discussion

An early cognitive change in PD is one of the most prevalent non-motor symptom and can even precede the PD's hallmark features. Early screening of cognitive impairment with sensitive instruments is required to

Table 2 Absolute effect size (|Cohen's d|) of subcortical regions

Region	HC versus PD-D	HC versus PD-MCI	NC-PD versus PD-D	PD-MCI versus PD-D
Right accumbens area	0.89	0.29	0.86	0.63
Left accumbens area	0.80	0.36	0.85	0.45
Right amygdala	0.48	0.07	0.51	0.46
Left amygdala	0.52	0.11	0.60	0.40
Right caudate	0.52	0.31	0.54	0.21
Left caudate	0.44	0.47	0.28	0.06
Right putamen	0.55	0.26	0.57	0.24
Left putamen	0.54	0.35	0.50	0.11
Right thalamus proper	0.55	0.28	0.80	0.90
Left thalamus proper	0.56	0.06	0.75	0.66

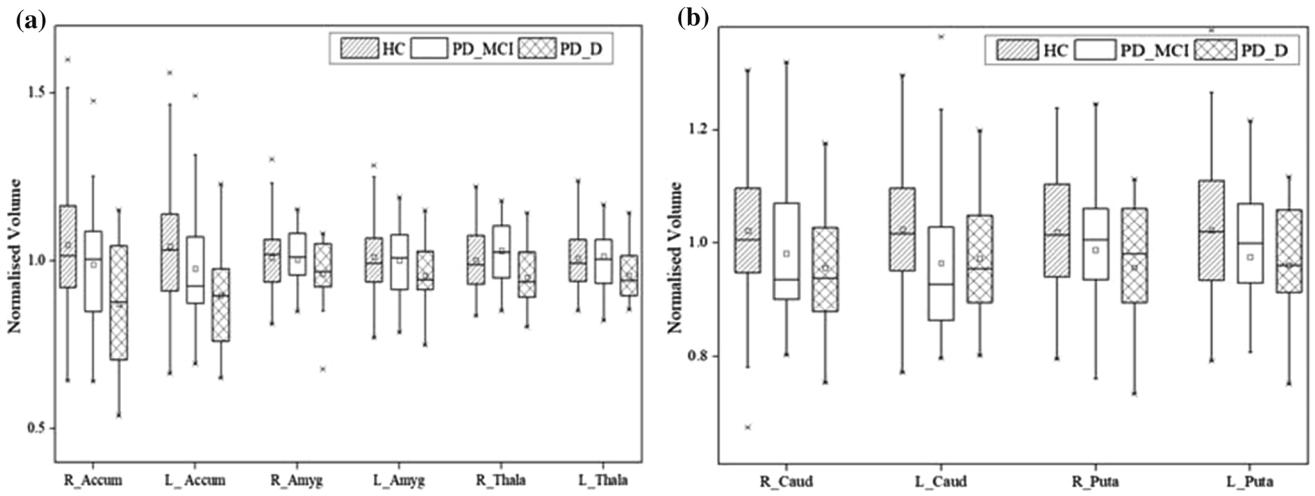

Fig. 4 Normalised volume of subcortical regions of HC, PD-MCI and PD-D subjects

diagnose the prevalence of dementia in PD and the conversion rate from MCI to PD-D. The objective of this study is to analyse the anatomical associations of the non-motor symptoms specific to the cognitive domain. The categorization of PD subjects under the distribution of various levels of cognitive impairment is based on the MoCA scores. Though MoCA is used as a global cognitive assessment tool, it lacks the diagnostic uncertainty in evaluating the progressive decline of nigrostriatal dopaminergic system and its association with the morphological changes (Delgado-Alvarado et al. 2016). The initial insight into the relationship of neuroimaging and subgrouping of PD subjects aid in early and objective diagnosis of PD.

The volumetric analysis of neuroanatomical structures is crucial in identifying the regional patterns of neurodegeneration underpinning cognitive dysfunction. Spatially localized multi atlas segmentation model is used for parallel segmentation of clinically relevant cortical structures. It has been proven that such approach involving automated segmentation and volume quantification of subcortical brain structures might be useful in both, research as well as clinical routine, to increase confidence in the diagnosis of neuro-degenerative disorders, such as Alzheimer's disease, Parkinson's disease. Further, it has also been suggested that utilization of more number of atlases helps in capturing structure-specific variation thereby enhancing segmentation accuracy (Wenzel et al. 2018). These recommendations are validated in the present study by using 45 manual atlases and 5111 auxiliary atlases accompanied by a set of neuroanatomical labels.

Volumetric analysis has been attempted in this study to describe the morphological variations related to PD. The comparison of TIV estimated from the segmented volumes illustrates only minimal volumetric changes and are not consistent with the levels of cognition in PD. The absence of changes in the gross measurement of the whole brain volumes required analysis of the localized volumetric alterations of subcortical structures across HC, PD-MCI and PD-D groups. The present study could confirm that disease-related atrophy can be found in a number of subcortical structures. The labelled subcortical structures are analysed to obtain the atrophy levels in the PD subjects with and without dementia.

The prediction of cognitive dysfunction in PD is evidenced through Cohen's d values of volumetric differences in accumbens, amygdala, caudate, putamen and thalamus. This observation is in line with the model based segmentation study by Wenzel et al. (2018) where a number of subcortical structures reflect neurodegenerative disease related atrophy, with amygdala and hippocampus being identified as the most relevant volumetric biomarkers. The volumetric differences of the caudate and putamen exhibited in this study play an important role in identification of cognitive impairment of PD subjects. The atrophy in these regions is also attributed to motor symptoms in the PD subjects as reported in a previous study (Li et al. 2018). The inverse association in the putamen and caudate with increasing motor severity in this early cohort of PD patients suggests early anterior striatal neurodegeneration. It has also been observed in another recent study where PD subjects with rapid eye movement sleep behaviour disorder demonstrated volumetric changes in the caudal putamen region (Kamps et al. 2019). In line with these findings, histologic studies in PD have shown prominent depletion of dopaminergic neurons in the caudal and lateral regions of the substantia nigra pars compacta, called nigrosome-1 (Pyatigorskaya et al. 2018).

The progression of the disease from MCI to later stages of cognitive decline is revealed through the volumetric

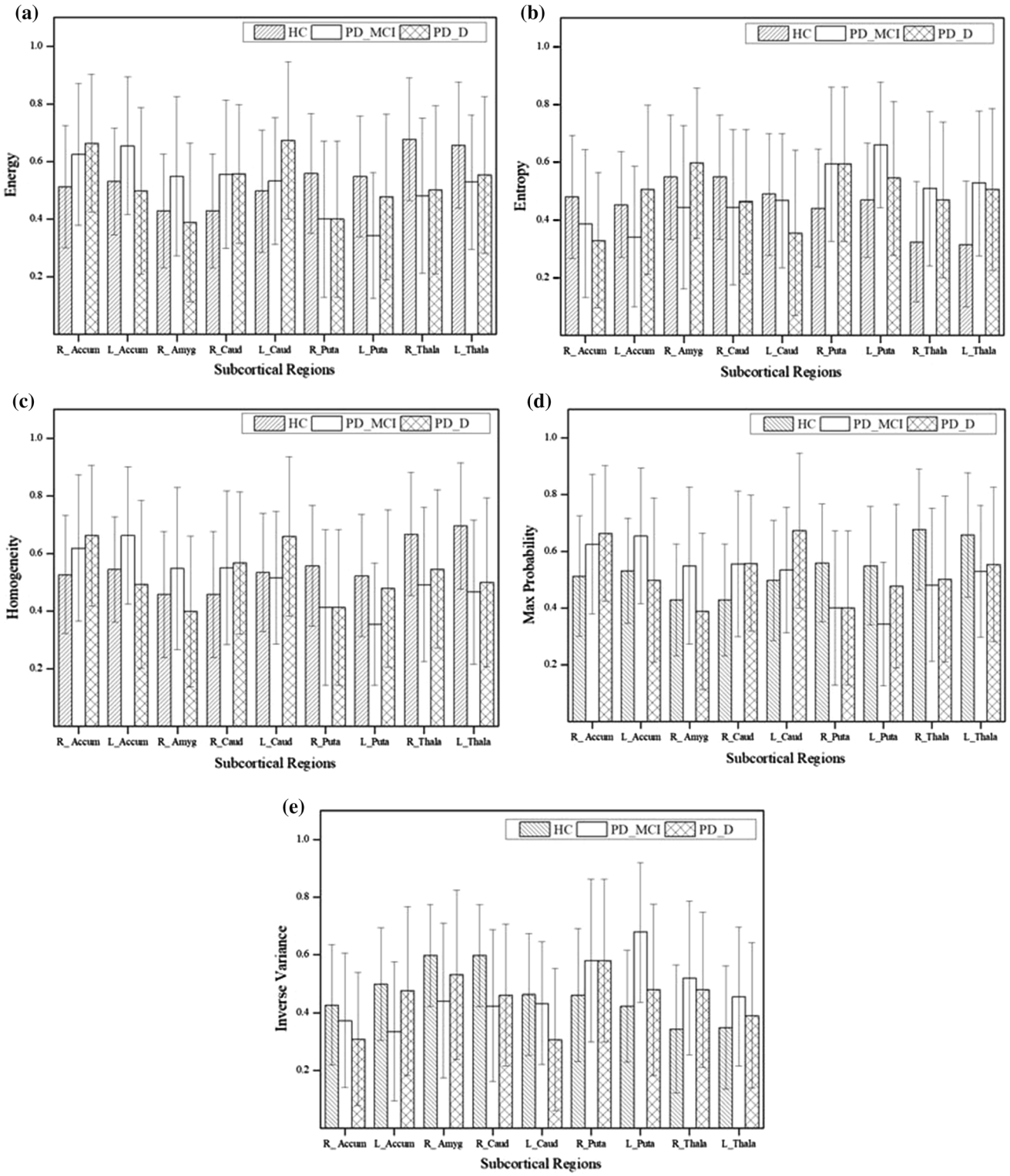

Fig. 5 Quantitative results of significant GLCM features **a** energy, **b** entropy, **c** homogeneity, **d** max probability, **e** inverse variance for the 9 significant regions subcortical regions

changes in the accumbens and thalamus with moderate and higher effect sizes respectively. It is observed that thalamus is largely affected in PD subjects with cognitive dysfunction. This is consistent with the previous studies demonstrating its association with depression in PD subjects (Garg et al. 2015). The significant volume reduction

Table 3 Performance measures of the classifier using texture features

Class	Accuracy (in %)	Sensitivity (in %)	Specificity (in %)
HC versus PD-MCI	88.3	82	95.5
HC versus PD-D	87.7	95.3	82.8
NC-PD versus PD-D	88.2	94.1	85.7
PD-MCI versus PD-D	96.2	96.5	96

of accumbens, amygdala, caudate, putamen and thalamus in the PD-D could be utilized to predict cognitive dysfunction in PD.

Minimal change in the subcortical volumes of the PD-MCI group is seen with an overlap in the volumetric estimates of the HC subjects. Though the results of present study proved to be able to discriminate PD-D patients from control subjects, it is found that the subcortical volumes are not the best parameters to characterize MCI in PD. Hence, morphological analysis using 3D GLCM has been attempted in this study. Similar results have been reported by Nemmi et al. (2015), where the modifications occurring in PD patients' subcortical structures are subtle and shape analysis techniques aiming at better identification of localized areas of brain atrophy, might be more sensitive to evidence such differences. It has also been reported by Wenzel et al. (2018) that modelling the variability of complex anatomies could better capture typical morphological variations of substructures that have different degree of atrophy in different brain structures.

The GLCM Haralick features extracted from the subcortical regions of the three subject groups exhibited volumetric differences with higher significance. Difference of significance in texture features from the co-occurrence matrix is seen between the right and left hemispheres as evidenced in the region of amygdala. This in line with the study carried out by Xia et al. (2013) to show the differences in the hemispherical levels as the disease progresses from mild to severe cognitive impairment. The region of interest derived morphometric values of each structure aids in discrimination among HC, NC-PD, PD-MCI and PD-D groups due to specific spatial localization.

The features from significant subcortical regions submitted to ensemble subspace kNN classifier achieved a comparable performance, in classifying the subjects as HC, PD-MCI and PD-D groups. The non-informative textural features of the entire data are handled by the ensemble classifier to obtain minimum error on classification. Specificity of 95.5 denotes the low probability of identifying the HC subjects as PD-MCI and proves the better discriminative capability of the classifier.

Conclusion

Cognitive impairment serves as significant clinical manifestation in PD. The cognitive impairment in PD subjects through morphological variation of subcortical structures has been analysed in this study. Multi-atlas based segmentation is implemented by combining deep neural networks with the native medical image processing techniques. The subcortical regions that exhibited medium and large effect sizes were evaluated through Cohen's d and these volumetric features exhibited the differences in structures of the three subject groups: HC, PD-MCI and PD-D. The comprehensive analysis of morphological alterations in the subcortical region could provide a sensitive evaluation for the assessment of cognitive dysfunction in PD. The diagnosis of PD-MCI still remains challenging, due to the overlap of subcortical volumes with the HC subjects and forms a scope for future validation in the early diagnosis of PD-MCI. The current study utilises the MoCA scores for the categorisation of subjects under the various cognitive levels. Inclusion of other neuropsychological tests would yield better categorisation of PD to access the early predictive capability of cognitive impairment.

Acknowledgements Data used in the preparation of this article were obtained from the Parkinson's Progression Markers Initiative (PPMI) database (www.ppmi-info.org/data). For up-to-date information on the study, visit www.ppmi-info.org. PPMI is a public-private partnership, funded by The Michael J. Fox Foundation for Parkinson's Research and funding partners, including AbbVie, Allergan, Amathus, Avid, Biogen, BioLegend, Bristol-Myers Squibb, Celgene, Denali, GE Healthcare, Genentech, GSK, Golub Capital, Handle Therapeutics, Insitro, Janssen Neuroscience, Lilly, Lundbeck, Merck, Meso Scale Discovery, Neurocrine, Pfizer, Piramal, Prevail Therapeutics, Roche, Sanofi Genzyme, Servier, Takeda, TEVA, UCB, Verily and Voyager Therapeutics (www.ppmi-info.org/fundingpartners).

Funding This work was supported by Anna Centenary Research Fellowship (Procs. No. CFR/ACRF/2018/AR1) offered by the Centre for Research, Anna University to S. Sivaranjini.

Declarations

Conflict of interest The Authors declares no conflict of interest.

References

Aarsland D (2016) Cognitive impairment in Parkinson's disease and dementia with Lewy bodies. Parkinsonism Relat Disord 22:S144–S148. https://doi.org/10.1016/j.parkreldis.2015.09.034

Amoroso N, La Rocca M, Monaco A, Bellotti R, Tangaro S (2018) Complex networks reveal early MRI markers of Parkinson's disease. Med Image Anal 48:12–24. https://doi.org/10.1016/j.media.2018.05.004

Babu GS, Suresh S, Mahanand BS (2014) A novel PBL-McRBFN-RFE approach for identification of critical brain regions responsible for Parkinson's disease. Expert Syst Appl 41:478–488. https://doi.org/10.1016/j.eswa.2013.07.073

Bermudez C, Plassard AJ, Chaganti S, Huo Y, Aboud KS, Cutting LE, Resnick SM, Landman BA (2019) Anatomical context improves deep learning on the brain age estimation task. Magn Reson Imaging 62:70–77. https://doi.org/10.1016/j.mri.2019.06.018

Chaudhary S, Kumaran SS, Kaloiya GS, Goyal V, Sagar R, Kalaivani M, Jaganathan NR, Mehta N, Srivastava A (2020) Domain specific cognitive impairment in Parkinson's patients with mild cognitive impairment. J Clin Neurosci 75:99–105. https://doi.org/10.1016/j.jocn.2020.03.015

Chaudhuri KR, Healy DG, Schapira AH (2006) Non-motor symptoms of Parkinson's disease: diagnosis and management. Lancet Neurol 5:235–245. https://doi.org/10.1016/S1474-4422(06)70373-8

Chou KL, Amick MM, Brandt J, Camicioli R, Frei K, Gitelman D, Goldman J, Growdon J, Hurtig HI, Levin B, Litvan I, Marsh L, Simuni T, Tröster AI, Uc EY (2010) A recommended scale for cognitive screening in clinical trials of Parkinson's disease. Mov Disord 25:2501–2507. https://doi.org/10.1002/mds.23362

Çiçek Ö, Abdulkadir A, Lienkamp SS, Brox T, Ronneberger O (2016) 3D U-Net: learning dense volumetric segmentation from sparse annotation. In: Ourselin S, Joskowicz L, Sabuncu M, Unal G, Wells W (eds) Medical image computing and computer-assisted intervention. Springer, Cham, pp 424–432. https://doi.org/10.1007/978-3-319-46723-8_49

Dadar M, Zeighami Y, Yau Y, Fereshtehnejad SM, Maranzano J, Postuma RB, Dagher A, Collins DL (2018) White matter hyperintensities are linked to future cognitive decline in de novo Parkinson's disease patients. NeuroImage Clin 20:892–900. https://doi.org/10.1016/j.nicl.2018.09.025

Dauer W, Przedborski S (2003) Parkinson's disease: mechanisms and models. Neuron 39:889–909. https://doi.org/10.1016/S0896-6273(03)00568-3

Delgado-Alvarado M, Gago B, Navalpotro-Gomez I, Jiménez-Urbieta H, Rodriguez-Oroz MC (2016) Biomarkers for dementia and mild cognitive impairment in Parkinson's disease. Mov Disord 31:861–881. https://doi.org/10.1002/mds.26662

Evans AC, Collins DL, Mills SR, Brown ED, Kelly RL, Peters TM (1993) 3D statistical neuroanatomical models from 305 MRI volumes. In: 1993 IEEE conference record nuclear science symposium and medical imaging conference, vol 3, pp 1813–1817

Folstein MF, Folstein SE, McHugh PR (1975) "Mini-mental state": a practical method for grading the cognitive state of patients for the clinician. J Psychiatr Res 2:189–198. https://doi.org/10.1016/0022-3956(75)90026-6

Garg A, Appel-Cresswell S, Popuri K, McKeown MJ, Beg MF (2015) Morphological alterations in the caudate, putamen, pallidum, and thalamus in Parkinson's disease. Front Neurosci 9:101. https://doi.org/10.3389/fnins.2015.00101

Gul A, Perperoglou A, Khan Z, Mahmoud O, Miftahuddin M, Adler W, Lausen B (2018) Ensemble of a subset of kNN classifiers. Adv Data Anal Classif 12:827–840. https://doi.org/10.1007/s11634-015-0227-5

Hall JM, Lewis SJ (2019) Neural correlates of cognitive impairment in Parkinson's disease: a review of structural MRI findings. Int Rev Neurobiol 144:1–28. https://doi.org/10.1016/bs.irn.2018.09.009

Heckemann RA, Hajnal JV, Aljabar P, Rueckert D, Hammers A (2006) Automatic anatomical brain MRI segmentation combining label propagation and decision fusion. Neuroimage 33:115–126. https://doi.org/10.1016/j.neuroimage.2006.05.061

Ho TK (1998) The random subspace method for constructing decision forests. IEEE Trans Pattern Anal Mach Intell 20:832–844. https://doi.org/10.1109/34.709601

Hoops S, Nazem S, Siderowf AD, Duda JE, Xie SX, Stern MB, Weintraub D (2009) Validity of the MoCA and MMSE in the detection of MCI and dementia in Parkinson disease. Neurology 73:1738–1745. https://doi.org/10.1212/WNL.0b013e3181c34b47

Hopes L, Grolez G, Moreau C, Lopes R, Ryckewaert G, Carrière N, Auger F, Laloux C, Petrault M, Devedjian JC, Bordet R, Defebvre L, Jissendi P, Delmaire C, Devos D (2016) Magnetic resonance imaging features of the nigrostriatal system: biomarkers of Parkinson's disease stages? PLoS ONE 11:e0147947. https://doi.org/10.1371/journal.pone.0147947

Hughes CP, Berg L, Danziger WL, Coben L, Martin RL (1982) A new clinical scale for the staging of dementia. Br J Psychiatry 140:566–572. https://doi.org/10.1192/bjp.140.6.566 (**PMID: 7104545**)

Huo Y, Xu Z, Aboud K, Parvathaneni P, Bao S, Bermudez C, Resnick SM, Cutting LE, Landman BA (2018) Spatially localized atlas network tiles enables 3D whole brain segmentation from limited data. In: Frangi A, Schnabel J, Davatzikos C, Alberola-López C, Fichtinger G (eds) Medical image computing and computer-assisted intervention. Springer, Cham, pp 698–705. https://doi.org/10.1007/978-3-030-00931-1_80

Huo Y, Xu Z, Xiong Y, Aboud K, Parvathaneni P, Bao S, Bermudez C, Resnick SM, Cutting LE, Landman BA (2019) 3D whole brain segmentation using spatially localized atlas network tiles. Neuroimage 194:105–119. https://doi.org/10.1016/j.neuroimage.2019.03.041

Kamps S, van den Heuvel OA, van der Werf YD, Berendse HW, Weintraub D, Vriend C (2019) Smaller subcortical volume in Parkinson patients with rapid eye movement sleep behavior disorder. Brain Imaging Behav 13:1352–1360. https://doi.org/10.1007/s11682-018-9939-4

Kletzel SL, Hernandez JM, Miskiel EF, Mallinson T, Pape TLB (2017) Evaluating the performance of the Montreal cognitive assessment in early stage Parkinson's disease. Parkinsonism Relat Disord 37:58–64. https://doi.org/10.1016/j.parkreldis.2017.01.012

Li X, Xing Y, Martin-Bastida A, Piccini P, Auer DP (2018) Patterns of grey matter loss associated with motor subscores in early Parkinson's disease. NeuroImage Clin 17:498–504. https://doi.org/10.1016/j.nicl.2017.11.009

Litvan I, Aarsland D, Adler CH, Goldman JG, Kulisevsky J, Mollenhauer B, Rodriguez-Oroz MC, Tröster AI, Weintraub D (2011) MDS task force on mild cognitive impairment in Parkinson's disease: critical review of PD-MCI. Mov Disord 26:1814–1824. https://doi.org/10.1002/mds.23823

Liu S, Yang H, Tong L, Liu W (2013) Detecting grey matter changes in preclinical phase of Alzheimer's disease by voxel-based morphometric and textural features: A preliminary study. In: 2013 IEEE third international conference on information science and technology (ICIST), pp 30–34. Doi: https://doi.org/10.1109/ICIST.2013.6747494

Marcus DS, Wang TH, Parker J, Csernansky JG, Morris JC, Buckner RL (2007) Open access series of imaging studies (OASIS): cross-sectional mri data in young, middle aged, nondemented, and demented older adults. J Cogn Neurosci 19:1498–1507. https://doi.org/10.1162/jocn.2007.19.9.1498

Marek K, Jennings D, Lasch S, Siderowf A, Tanner C, Simuni T, Coffey C, Kieburtz K, Flagg E, Chowdhury S, Poewe W (2011) The Parkinson progression marker initiative (PPMI). Prog Neurobiol 95:629–635. https://doi.org/10.1016/j.pneurobio.2011.09.005

Milletari F, Ahmadi SA, Kroll C, Plate A, Rozanski V, Maiostre J, Levin J, Dietrich O, Ertl-Wagner B, Bötzel K, Navab N (2017) Hough-CNN: deep learning for segmentation of deep brain regions in MRI and ultrasound. Comput Vis Image Underst 164:92–102. https://doi.org/10.1016/j.cviu.2017.04.002

Nasreddine ZS, Phillips NA, Bédirian V, Charbonneau S, Whitehead V, Collin I, Cummings JL, Chertkow H (2005) The Montreal cognitive assessment, MoCA: a brief screening tool for mild cognitive impairment. J Am Geriatr Soc 53:695–699. https://doi.org/10.1111/j.1532-5415.2005.53221.x

Nemmi F, Sabatini U, Rascol O, Péran P (2015) Parkinson's disease and local atrophy in subcortical nuclei: insight from shape analysis. Neurobiol Aging 36:424–433. https://doi.org/10.1016/j.neurobiolaging.2014.07.010

Poewe W, Seppi K, Tanner CM, Halliday GM, Brundin P, Volkmann J, Schrag AE, Lang AE (2017) Parkinson disease. Nat Rev Dis Prim 3:17013. https://doi.org/10.1038/nrdp.2017.13

Provost JS, Hanganu A, Monchi O (2015) Neuroimaging studies of the striatum in cognition part I: healthy individuals. Front Syst Neurosci 9:140. https://doi.org/10.3389/fnsys.2015.00140

Pyatigorskaya N, Magnin B, Mongin M, Yahia-Cherif L, Valabregue R, Arnaldi D, Ewenczyk C, Poupon C, Vidailhet M, Lehéricy S (2018) Comparative study of MRI biomarkers in the substantia nigra to discriminate idiopathic Parkinson disease. Am J Neuroradiol 39:1460–1467. https://doi.org/10.3174/ajnr.A5702

Rektorova I, Biundo R, Marecek R, Weis L, Aarsland D, Antonini A (2014) Grey matter changes in cognitively impaired Parkinson's disease patients. PLoS ONE 9:e85595. https://doi.org/10.1371/journal.pone.0085595

Salvatore C, Cerasa A, Castiglioni I, Gallivanone F, Augimeri A, Lopez M, Arabia G, Morelli M, Gilardi MC, Quattrone A (2014) Machine learning on brain MRI data for differential diagnosis of Parkinson's disease and progressive supranuclear palsy. J Neurosci Methods 222:230–237. https://doi.org/10.1016/j.jneumeth.2013.11.016

Simuni T, Caspell-Garcia C, Coffey CS, Weintraub D, Mollenhauer B, Lasch S, Tanner CM, Jennings D, Kieburtz K, Chahine LM, Marek K (2018) Baseline prevalence and longitudinal evolution of non-motor symptoms in early Parkinson's disease: the PPMI cohort. J Neurol Neurosurg Psychiatry 89:78–88. https://doi.org/10.1136/jnnp-2017-316213

Tustison NJ, Avants BB, Cook PA, Zheng Y, Egan A, Yushkevich PA, Gee JC (2010) N4ITK: improved N3 bias correction. IEEE Trans Med Imaging 29:1310–1320

Wenzel F, Meyer C, Stehle T, Peters J, Siemonsen S, Thaler C, Zagorchev L (2018) Rapid fully automatic segmentation of subcortical brain structures by shape-constrained surface adaptation. Med Image Anal 46:146–161. https://doi.org/10.1016/j.media.2018.03.001

Wolters AF, Moonen AJH, Lopes R, Leentjens AFG, Duits AA, Defebvre L, Delmaire C, Hofman PA, van Bussel FC, Dujardin K (2020) Grey matter abnormalities are associated only with severe cognitive decline in early stages of Parkinson's disease. Cortex 123:1–11. https://doi.org/10.1016/j.cortex.2019.09.015

Xia J, Miu J, Ding H, Wang X, Chen H, Wang J, Wu J, Zhao J, Huang H, Tian W (2013) Changes of brain gray matter structure in Parkinson's disease patients with dementia. Neural Regen Res 8:1276–1285. https://doi.org/10.3969/j.issn.1673-5374.2013.14.004

Yesavage JA, Brink TL, Rose TL, Lum O, Huang V, Adey M, Leirer VO (1983) Development and validation of a geriatric depression screening scale: a preliminary report. J Psychiatr Res 17:37–49. https://doi.org/10.1016/0022-3956(82)90033-4